**INTERNATIONAL COUNCIL FOR RESEARCH AND INNOVATION
IN BUILDING AND CONSTRUCTION**

WORKING COMMISSION W18 - TIMBER STRUCTURES

DESIGN OF SHEAR REINFORCEMENT FOR TIMBER BEAMS

P Dietsch

H Kreuzinger

S Winter

Lehrstuhl für Holzbau und Baukonstruktion

Technische Universität München

GERMANY

Pesented by P Dietsch

P Dietsch discussed the question whether the thesis covered cases where shear cracks followed a step pattern and did not follow a horizontal line. P Dietsch stated the model could consider such cases however friction could come into play in a step pattern which would not be considered.

M Fragiacomo stated it would be a good idea to pre-stress. P Dietsch stated that pre-stressing could be lost due to creep. M Fragiacomo suggested using a spring to maintain pre-stressing. P Dietsch stated this might not be the best idea.

A Frangi questioned whether minimum stiffness of the screw can be given. P Dietsch stated that a general method was presented without presenting a minimum value. He further discussed results from TU Munich and Karlsruhe Institute of Technology where different connectors were considered and large glued in rods achieved higher stiffness compared to self-tapping wood screws. H Blass commented that stiffness per unit length should be considered. P Dietsch commented that 45 degree inclined screw angle made the best option for shear reinforcement.

F Lam asked about availability of information for stiffness as a function of inclined angle. P Dietsch responded that not much information is available although the Karlsruhe data indicated a trend that the stiffness increased as the angle decreased.

U Kuhlmann stated that rehabilitation of existing structures could be an interesting field of study. P Dietsch agreed and stated there are many practical examples for such applications.

M Fragiacomo asked whether one can achieve full capacity using screws to reinforce a fully cracked beam. P Dietsch stated very close screw spacing would be needed to achieve full capacity.

Design of shear reinforcement for timber beams

P. Dietsch, H. Kreuzinger, S. Winter

Lehrstuhl für Holzbau und Baukonstruktion

Technische Universität München, Germany

1 Introduction and objective

The use of glulam beams with changing depth offers the possibility to adapt the section modulus to the bending moment. In the case of single-span beams under uniformly distributed load, however, a change in beam depth will lead to a contrary effect for the shear stresses, see Figure 1. Curved and pitched cambered beams feature not only high utilization rates in bending but also areas of high tension stresses perpendicular to the grain and shear parallel to the grain stresses, two stress components for which timber features only small capacities as well as brittle failure modes. Out of 245 cases of damaged or failed large-span timber structures, evaluated in [1], several failures document the possibility of a shear fracture (full separation) developing in grain direction from the curved part towards the supports, partly followed by a failure of the beam in flexural tension due to a change in stress distribution resulting from the change in section modulus. Reinforcements against tension stresses perpendicular to the grain in form of fully threaded screws or threaded rods can be considered state of the art [2], [3]. With respect to their application as shear reinforcement, not many research results are yet available [4], [5], resulting in a lack of experimentally validated design approaches.
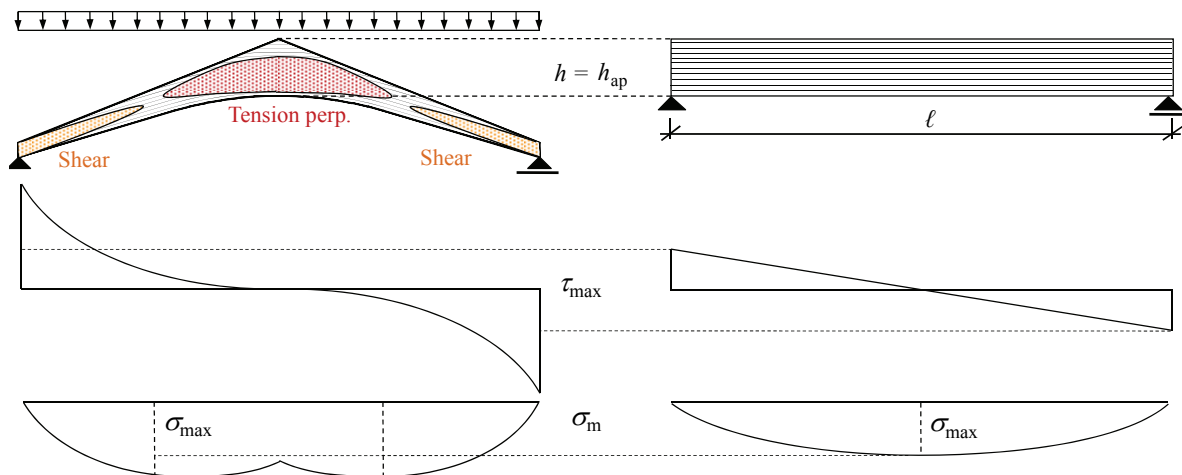

Figure 1: Schematic illustration of the distribution of shear stresses and bending stresses in straight beam and pitched cambered beam

Most approaches to design reinforcement against tension stresses perpendicular to the grain assume that the stresses are entirely carried by the reinforcement [2], [3]. However, with respect to an economic use of reinforcing elements it is of interest, whether a proportionate distribution of shear stresses between the timber beam and the shear reinforcement can be achieved in the unfractured state. This is particularly relevant, if a high number of reinforcing elements is necessary to achieve the full design capacity of the timber beam. For timber, the shear strength is in the range of five times the magnitude of tension perpendicular to the grain strength.

Within this paper, approaches to design shear reinforcement for glulam beams in the unfractured and the fractured state are presented, validated and discussed. The moment of failure, i.e. the transition from the unfractured to the fractured state is characterized by dynamic effects. This situation is not covered in this paper. A possible approach is given in [1]. The same applies to the subject of moisture induced stresses, resulting from the reinforcement restricting the free shrinkage or swelling of the glulam beam.

2   Design of shear reinforcement for the unfractured state

2.1   Analytical approach

In the following, an analytical approach is presented which allows calculating the effectivity of shear reinforcement in the unfractured state (see also [6]). Using matrix format, the approach is based on common theoretical concepts and constitutive equations for material properties. It considers the structural anisotropy of the cross-sections with shear reinforcement and enables to incorporate the semi-rigid composite action between the reinforcement and the wood material. The stresses caused by the shear forces are used to determine the shear strains which are in turn used to determine the stresses in the reinforcement and in the timber beam.

The approach is applicable to structural members featuring uniaxial load transfer and - within segments of the member - a uniform arrangement of reinforcing elements and uniform shear stress. The latter is given for beams under concentrated loads and correspondingly segment-wise constant shear stress. In the case of beams under uniform load, featuring common length to depth ratios, an adequate approximation can be assumed. For areas close to the supports ($0 \leq x \leq h$ from the support), separate investigations have to be carried out, if necessary. In the case of direct supports, the area close to the supports is subjected to compression stresses perpendicular to the grain, resulting in an increased shear capacity of the timber beam in this area [7].

The approach is based on the theory for composite materials. In [8] (and on the basis of [9] and [10]), anisotropic material properties of composite materials were derived for the example of laminated timber elements under in-plane loading and in bending. The orientation of the different layers of boards is accounted for; the effect of the composite action is described. In [11], these material properties were used in combination with the theory of composite materials to conduct numerical calculations on walls made of cross-laminated timber. The derivation of stiffness coefficients for individual layers with different orientation to enable a calculation of the overall stiffness of the system under consideration [8] can be transferred to reinforcement in timber elements.

According to the law of elasticity, the stress-strain-relationship of an element under in-plane loading in the *x*-*z*-plane (see Figure 2) is: $\varepsilon = S \cdot \sigma$. Inverting the matrix *S* leads to the stiffness matrix *C*, enabling to determine the resulting stresses due to known strains:

$$\begin{vmatrix} \sigma_x \\ \sigma_z \\ \tau_{xz} \end{vmatrix} = \begin{vmatrix} C_{11} & C_{12} & C_{13} \\ C_{21} & C_{22} & C_{23} \\ C_{31} & C_{32} & C_{33} \end{vmatrix} \cdot \begin{vmatrix} \varepsilon_x \\ \varepsilon_z \\ \gamma_{xz} \end{vmatrix} \quad \text{resp.} \quad \sigma = C \cdot \varepsilon = S^{-1} \cdot \varepsilon \tag{1}$$

Regarding a composite section, featuring two or more layers of structural elements with different orientations, the stiffness matrices of the individual layers have to be transformed into a global coordinate system. Using the global stiffness matrix, loads can be applied on the composite section. Based on this, the resulting strains are determined, which are in turn

used to determine the stresses in the individual layers of structural elements. The procedure is shown schematically in Figure 2. Since the local coordinate system of layer 1 coincides with the global coordinate system, neither a transformation of its stiffness matrix (C_1), nor of the strains determined for the global system (ε_0) is required. Therefore, for the calculation of the global stiffness matrix, only the stiffness matrix of layer 2 (C_2) has to be transformed into the global system. According to the law of elasticity, the strains (ε_0) of the composite section can be determined by a multiplication of the inverse global stiffness matrix (C_0^{-1}) with a load vector (n_0). To determine the stresses in layer 2 (n_2), the strains in the global system have to be rotated into the local coordinate system of layer 2.

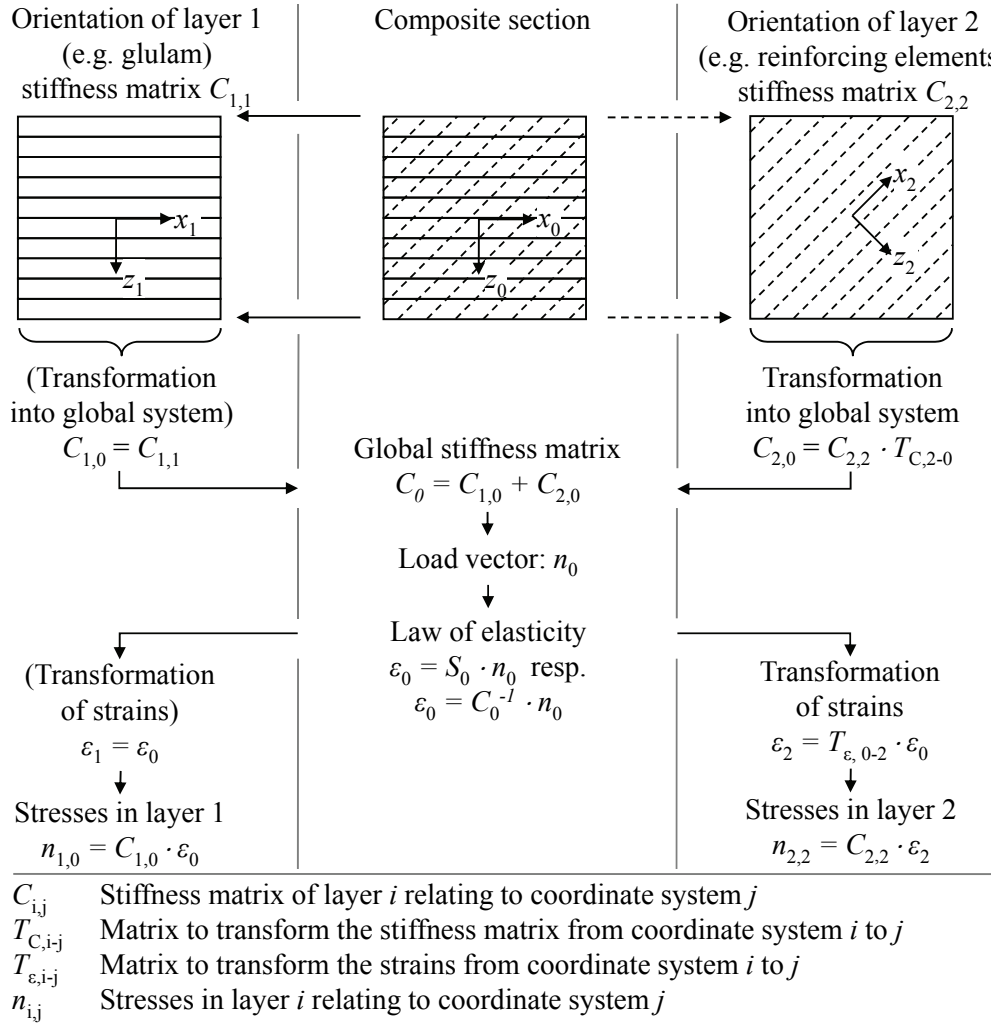| $C_{i,j}$ | Stiffness matrix of layer i relating to coordinate system j |
$T_{C,i\text{-}j}$	Matrix to transform the stiffness matrix from coordinate system i to j
$T_{\varepsilon,i\text{-}j}$	Matrix to transform the strains from coordinate system i to j
$n_{i,j}$	Stresses in layer i relating to coordinate system j

Figure 2: Calculation procedure based on the structural anisotropy

2.2 Application to shear reinforcement

The before explained method can also be applied to glulam elements (and cross-laminated timber (CLT) elements) featuring shear reinforcement, see [6]. For simplification, the global coordinate system should be matched with the local coordinate system of the timber section, see Figure 3.

Considering the coordinates and angular relationships defined in Figure 3, the stiffness coefficients of the reinforcing elements can be transformed into the global system, following common mechanical rules (see e.g. Equation 3 and [6]). The same is valid for the strains in the reinforcing elements which are determined by transforming the strains in the global system into the local coordinate system (see e.g. Equation 9 and [6]).
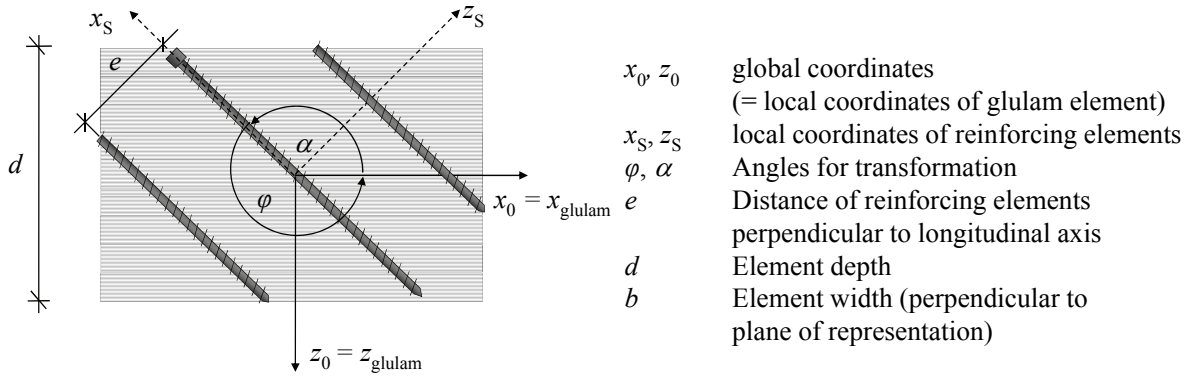
Figure 3: Denomination of coordinates and angles for the transformation of stiffness parameters within the structural anisotropy

2.2.1 Determination of stiffness parameters in the global system

When determining the global stiffness, the cross-sectional layup of the structural element to be reinforced has to be considered. In the case of glulam elements, constant material properties are assumed in direction of the global coordinates, meaning that the stiffness matrix of the glulam element, $C_{GL,0}$, is a result of the material parameters in the respective directions. Due to the lack of precise data for wood and for purposes of simplification, the Poisson's ratio μ is set to zero.

$$C_{GL,0} = \begin{vmatrix} E_0 & 0 & 0 \\ 0 & E_{90} & 0 \\ 0 & 0 & G \end{vmatrix} \tag{2}$$

Assuming that the shear reinforcement in the form of threaded rods or fully threaded screws is primarily loaded in axial direction, the axial stiffness EA_S of the reinforcement is essential with respect to the load bearing behavior. The bending stiffness has a minor effect and is therefore neglected for reasons of simplification. By means of the transformation matrix, the stiffness matrix of the reinforcement with respect to the global system, $C_{S,0}$, can be determined as follows:

$$C_{S,0} = \left(\frac{n_s}{b} \cdot \frac{EA_S}{e} \right) \cdot T_{C,S-0} = \left(\frac{n_s}{b} \cdot \frac{EA_S}{e} \right) \cdot \begin{vmatrix} \cos^4 \varphi & \sin^2 \varphi \cdot \cos^2 \varphi & -\sin \varphi \cdot \cos^3 \varphi \\ \sin^2 \varphi \cdot \cos^2 \varphi & \sin^4 \varphi & -\sin^3 \varphi \cdot \cos \varphi \\ -\sin \varphi \cdot \cos^3 \varphi & -\sin^3 \varphi \cdot \cos \varphi & \sin^2 \varphi \cdot \cos^2 \varphi \end{vmatrix} \tag{3}$$

with:
EA_S Axial stiffness of the reinforcing elements
n_S number of rows of reinforcing elements perpendicular to loaded plane

The total stiffness of the composite section in the global system, C_0, is determined by adding the stiffness matrices of the glulam element, $C_{GL,0}$, and the reinforcement, $C_{S,0}$.

$$C_0 = C_{GL,0} + C_{S,0} \tag{4}$$

2.2.2 Determination of stresses

The load on a reinforced timber element can be introduced by means of the vector n_0. The vector contains the stresses σ_{x0} and σ_{z0} in the main axes of the global system as well as the shear stresses τ_{xz0} in the x-z-plane. The stresses applied by the vector n_0 are constant in the segment under consideration. The strains resulting from the given stresses are determined by multiplying the vector n_0 with the inverse stiffness matrix C_0^{-1}:

$$\varepsilon_0 = C_0^{-1} \cdot n_0 \tag{5}$$

Due to the differently oriented local coordinate systems, the strains determined for the global system are used to separately determine the stresses in the glulam element and the shear reinforcement.

Glulam element:

Since the local coordinates of the glulam element coincide with the global coordinates, no transformation of the strains is necessary when determining the stresses.

$$n_{GL} = C_{GL,0} \cdot \varepsilon_{GL} = C_{GL,0} \cdot \varepsilon_0 \tag{6}$$

A comparison between the shear stresses in the global system τ_{xz0} and the resulting shear stresses in the glulam element $\tau_{GL,xz0}$ delivers the degree of strengthening η_τ, which describes the reduction in shear stress due to the reinforcement.

$$\eta_\tau = \frac{\tau_{xz_0}}{\tau_{GL,xz_0}} \tag{7}$$

In addition, Equation (6) delivers the normal stress component $\sigma_{GL,z0}$. If the arrangement is chosen so that the shear reinforcement is loaded in axial tension, the resulting stresses in the glulam element are in compression perpendicular to the grain. Several experimental investigations, e.g. [12], [13], [14] have shown, that compression stresses perpendicular to the grain have a positive effect on the shear capacity. This means that the shear reinforcement leads not only to a reduction of shear stresses in the timber but, in the case of appropriate arrangement, to a stress interaction which has a positive effect on the shear capacity of the glulam element. In [4], based on the results given in [12], the following equation is proposed:

$$\tau = 4.75\,N/mm^2 - 1.15 \cdot \sigma_\perp - 0.13 \cdot \sigma_\perp^2 \qquad \lfloor N/mm^2 \rfloor \tag{8}$$

Shear reinforcement:

The stresses in the shear reinforcement are determined by transforming the strains in the global coordinate system into the local coordinate system of the shear reinforcement. Since only the axial stiffness EAs of the shear reinforcement is considered, it is sufficient to calculate the strain parallel to the axis of load transfer of the reinforcement.

$$\varepsilon_S = \varepsilon_0 \cdot T_{\varepsilon,0-S} \quad \text{here:} \quad \varepsilon_{x_S} = \begin{vmatrix} \varepsilon_{x_0} \\ \varepsilon_{z_0} \\ \gamma_{xz_0} \end{vmatrix} \cdot \begin{vmatrix} \cos^2\alpha & \sin^2\alpha & \sin\alpha \cdot \cos\alpha \end{vmatrix} \tag{9}$$

The stresses in the axis of the reinforcement σ_S in each reinforcing element are:

$$\sigma_{S,x_S} = \varepsilon_{x_S} \cdot E_S \tag{10}$$

2.2.3 Incorporation of the semi-rigid composite action between the reinforcement and the wood material

In the determination of the global stiffness matrix C_0, see 2.2.1, a rigid bond between the shear reinforcement and the glulam element is assumed. This is approximately the case, if glued-in rods are applied, see e.g. [15]. Reinforcing with pre-drilled, screwed-in threaded rods or fully threaded screws leads to a semi-rigid composite action between the wood material and the thread of the reinforcement. It is therefore necessary to take into account that different strains occur in the timber section and the reinforcement. The semi-rigid

composite action can be incorporated by an embedment modulus (modulus of foundation). This can be determined from appropriate tests, see e.g. [16].

Alternatively it is possible to describe the semi-rigid composite action with the axial slip modulus $K_{ax,ser}$, which is usually included in the technical approvals of fully threaded screws or threaded rods. This is comparable to a spring stiffness and enables to determine the relative displacement between an axially loaded screw or rod and the wood surface.

The axial slip modulus $K_{ax,ser}$ is only of limited suitability for the method presented, since it does not provide information about the distribution of shear stresses in the embedding wood material and the resulting distribution of normal forces in the reinforcing element. However, it is possible to deduce an embedment modulus from the coefficient $K_{ax,ser}$. For this purpose, the load-bearing behavior of the reinforcement can be described by an equivalent mechanical system that consists of an elastically (in the direction of the reinforcement) supported beam, see Figure 4.
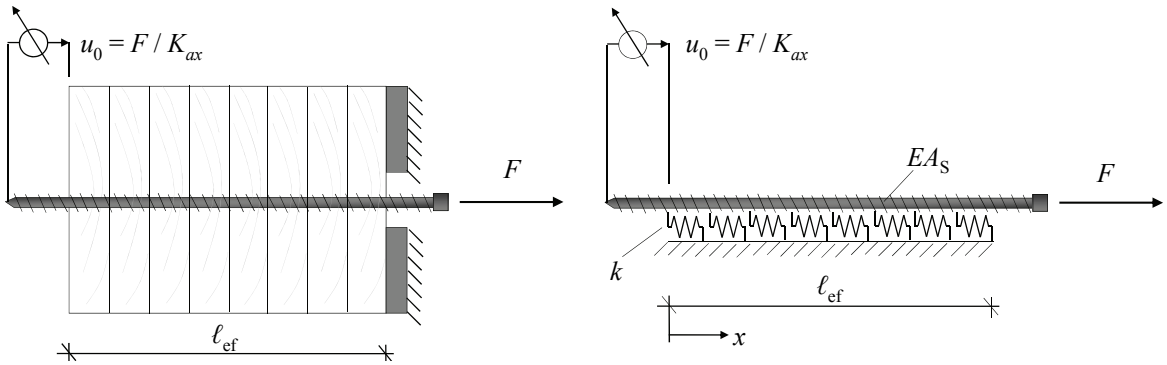

Figure 4: Experimental setup to determine K_{ax} [17] and equivalent mechanical system

The general approach for the homogeneous solution of the differential equation of the beam on horizontally elastic foundation is:

$$u_{(x)} = C_1 \cdot e^{\lambda \cdot x} + C_2 \cdot e^{-\lambda \cdot x} \quad \text{with:} \quad \lambda = \sqrt{k / EA_S} \tag{11}$$

Taking into account the present boundary conditions, the following solution for the differential equation can be obtained:

$$\lambda \cdot \left(e^{\lambda \cdot l_{ef}} - e^{-\lambda \cdot l_{ef}} \right) = 2 \cdot K_{ax} / EA_S \tag{12}$$

The coefficient λ can be determined iteratively or by using appropriate software. Subsequently the embedment modulus k, can be calculated with Equation 13.

$$k = \lambda^2 \cdot EA_S \tag{13}$$

Values for the axial slip modulus $K_{ax,ser}$, given in literature or technical approvals, are generally valid for angles of 90° between the screw or rod axis and the grain direction (as shown in Figure 4. In the case of shear reinforcement, the typically applied angle is 45° (as shown in Figure 5). In [4], axial slip moduli were determined for screwed-in threaded rods of $d = 16$ mm and 20 mm, penetration lengths of 200 mm and 400 mm and angles between the rod axis and the grain direction of 45° and 90°. For angles of 45°, higher axial slip moduli are determined. In addition, a disproportionate (above-average) increase of the axial stiffness is determined when doubling the penetration length. When applying these values within the analytical method, it should be considered that the applicable length l_{ef} corresponds to half the length of the reinforcing element, see Figure 5.
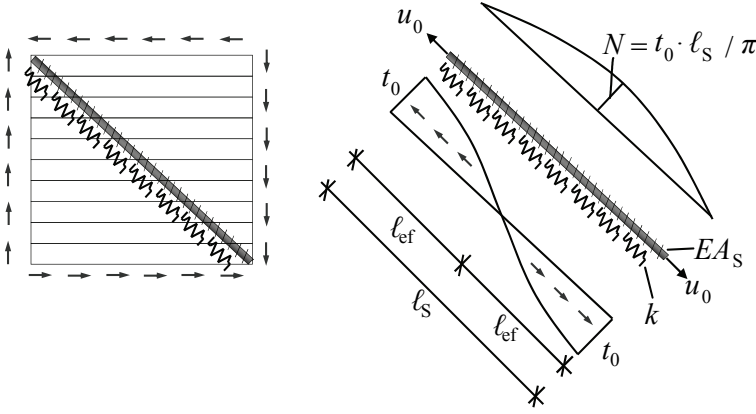
Figure 5: Semi-rigid composite between reinforcement and the wood material

Different methods exist to account for the semi-rigid composite action between two structural elements. One common approach in structural timber design is the γ-method [7]. This method is mostly applied to timber-concrete composite elements or mechanically jointed beams, however it can be extended in order to utilize it for the semi-rigid composite action of shear reinforcements. In this case, the relationships given in Figure 5 apply.

Assuming that the shear deformation of the glulam element will approximately result in a sinusoidal distribution of axial force in the reinforcement, the distribution of shear flow in the embedment has to follow cosinusoidal form. The deformation u_0 is a combination of the deformations in the composite and in the reinforcement under normal force.

$$u_0 = \frac{t_0}{k} + t_0 \cdot \frac{(2 \cdot l_{ef})^2}{\pi^2} \cdot \frac{1}{EA_S} \tag{14}$$

The deformation of a reinforcing element with an effective axial stiffness $efEA_S$ under given load, and without consideration of the elastic foundation, is calculated as follows:

$$u_0 = t_0 \cdot \frac{(2 \cdot l_{ef})^2}{\pi^2} \cdot \frac{1}{efEA_S} \tag{15}$$

Combining Equations (14) and (15), the effective axial stiffness $efEA_S$ is obtained:

$$efEA_S = EA_S \cdot \frac{1}{1 + \dfrac{\pi^2 \cdot EA_S}{(2 \cdot l_{ef})^2 \cdot k}} = EA_S \cdot \gamma \tag{16}$$

In analogy to the γ-method, the axial stiffness of the reinforcing element can be reduced by the factor γ to account for the semi-rigid composite action. For the stiffness matrix of the reinforcement with respect to the global system, the following applies:

$$C_{S,0} = \left(\frac{n_s}{b} \cdot \frac{efEA_S}{e} \right) \cdot T_{C,S-0} = \left(\frac{n_s}{b} \cdot \frac{\gamma \cdot EA_S}{e} \right) \cdot T_{C,S-0} \tag{17}$$

The semi-rigid composite action leads to the following equation to determine the axial stresses $\sigma_{S,xs}$ in each reinforcing element:

$$\sigma_{S,x_S} = \varepsilon_{x_S} \cdot \gamma \cdot E_S \tag{18}$$

$$N_{S,x_S} = \varepsilon_{x_S} \cdot \gamma \cdot EA_S \tag{19}$$

with: factor γ according to Equation (16)

2.3   Comparison with experimental tests

To validate the design method for shear reinforcement in the unfractured state, experiments on glulam beams, shear reinforced with fully threaded screws were performed. First, non-destructive tests, according to EN 408 [18], were performed in the linear-elastic range to determine the effective shear stiffness of the reinforced glulam beams. The same specimen was tested several times, while its properties (reinforcement) were changed between the experiments. Cracks were introduced in half of the twelve glulam specimens, to study a potential increase in the effect of the reinforcement in cracked members. After assessing the pros and cons of introducing cracks through drying processes or mechanically (in which the wood fibers are cut locally), latter option was chosen since only in this case, the depth of the crack and remaining cross-section can clearly be defined. After testing all specimens without shear reinforcement, two configurations of shear reinforcement (at a distance of 160 mm and 80 mm) were applied and tested, see Figure 6. For this, fully threaded screws, featuring a diameter $d = 8$ mm and a length $\ell_S = 280$ mm were used [19].
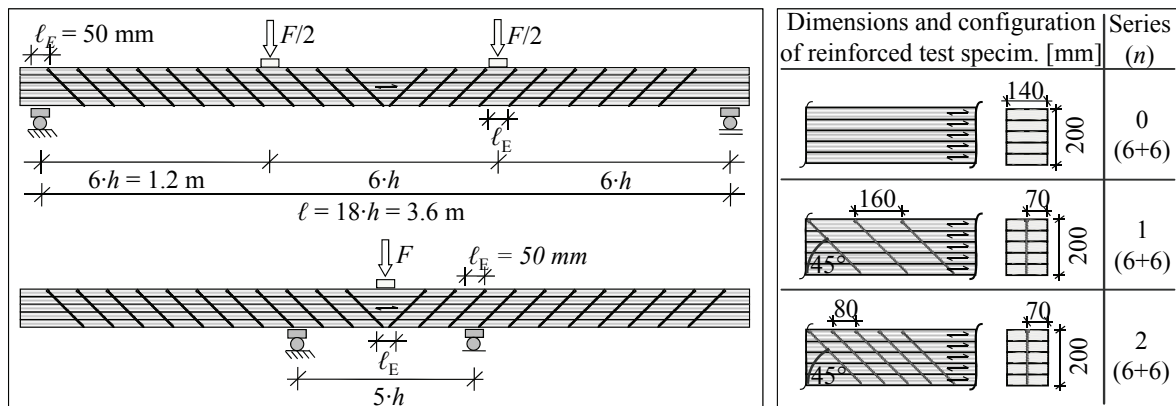

Figure 6: Experimental tests to determine the effective shear modulus G of glulam elements with fully threaded screws as shear reinforcement - experimental setup and geometry

Based on the data obtained from the unreinforced elements, the expected effective shear modulus G was determined for the reinforced elements by means of the analytical method. The embedment modulus k of the reinforcement was derived from test results for fully threaded screws in glulam, given in [4] and [20]. The increase of the effective shear modulus G, determined from tests and analytical calculations, was for all configurations in the single digit percentage range. The results of the analytical calculations and the experimental results are compared in Figure 7. The compression perpendicular to the grain stresses induced into the glulam element by the reinforcement were too small to have a positive influence in terms of the stress interaction between shear and compression perpendicular to the grain.

The test results confirm the small effect of the reinforcing elements on the shear stiffness (see also [5]) and hence the low transfer of shear from the glulam beams to the shear reinforcement in the unfractured state. The reduction of shear stiffness due to the cracks could clearly be seen. For the second level of reinforcement, no further increase of the effective shear modulus could be observed. Comparative experiments to study a potential reduction of the axial slip modulus $K_{ax,ser}$ in the case of repeated loading could not confirm this possibility. On the contrary, an improvement of stiffness of the composite between reinforcement and the wood material was found in the case of repeated loading [1]. A possible explanation can be concluded from the known sensitivity of the shear modulus G to the apparent modulus of elasticity $E_{app,}$ see [21], which has to be determined at small span $\ell = 5 \cdot h$ (see Figure 6 lower part) and hence small deformations w and high loads F.

A comparison with two other methods to determine the shear modulus (dynamic response, shear field) showed that the applied bending method returned the most acceptable accuracy.
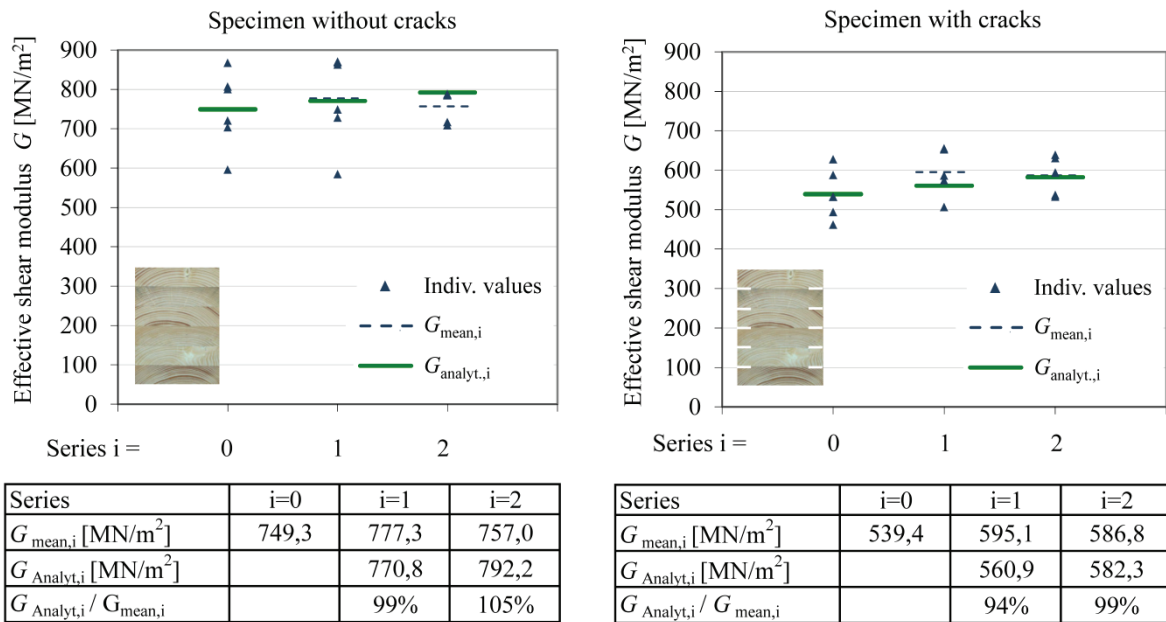
Specimen without cracks

Series	i=0	i=1	i=2
$G_{mean,i}$ [MN/m^2]	749,3	777,3	757,0
$G_{Analyt,i}$ [MN/m^2]		770,8	792,2
$G_{Analyt,i}$ / $G_{mean,i}$		99%	105%

Specimen with cracks

Series	i=0	i=1	i=2
$G_{mean,i}$ [MN/m^2]	539,4	595,1	586,8
$G_{Analyt,i}$ [MN/m^2]		560,9	582,3
$G_{Analyt,i}$ / $G_{mean,i}$		94%	99%

Figure 7: Effective shear modulus G of glulam beams with and without cracks at different levels of shear reinforcement – comparison of analytical approach with experimental results

After the non-destructive tests in the linear-elastic range had been completed, the beams were cut into smaller segments. By removing some of the screws, three different configurations of reinforcement could be realized with at least ten specimens for each configuration, see Figure 8. The destructive tests to determine the shear strength of each series were carried out again on the basis of EN 408 [18], see Figure 8.
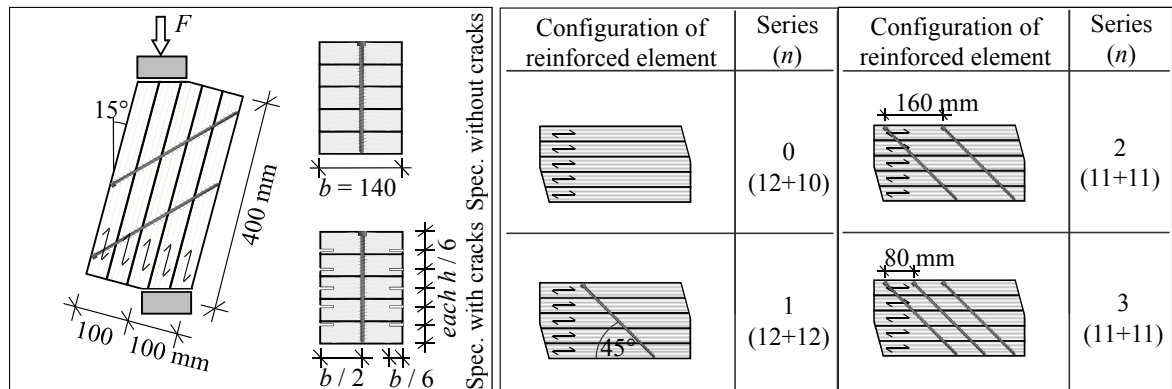
Configuration of reinforced element	Series (n)	Configuration of reinforced element	Series (n)
	0 (12+10)	160 mm	2 (11+11)
45°	1 (12+12)	80 mm	3 (11+11)

Figure 8: Experimental tests to determine the shear strength f_v of glulam elements with self-tapping screws as shear reinforcement – experimental setup and geometry

The experimental and analytical results were in accordance with abovementioned finding. Again, the increase in shear strength was only in the single digit percentage range, see Figure 9. Here, the influence of compression stresses perpendicular to the grain on the shear capacity was taken into account using the abovementioned proposal. The increase in shear strength determined in the tests correlates well with the tensile load-carrying capacity of the screws in direction of the shear plane [4]. For the specimens featuring more reinforcing elements (series 2 and 3), a resumption of load-carrying capacity could be observed at lower load-level after the shear fracture. Here, after fracture, the load was

carried by the screws. The activation of friction led to an additional load-carrying capacity. The shear strength of specimens with cracks was on average 14% lower than that for the specimens without cracks. The reason is believed the local weakening of the cross-section due to the local cutting of the wood fibers when introducing the cracks mechanically.
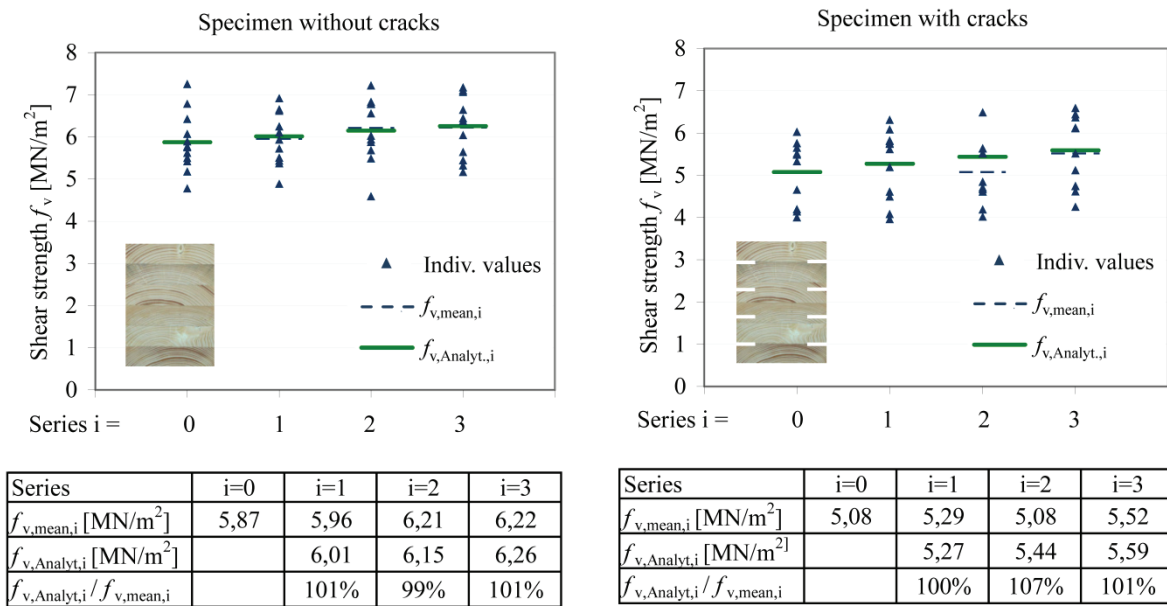

Series	i=0	i=1	i=2	i=3
$f_{v,mean,i}$ [MN/m^2]	5,87	5,96	6,21	6,22
$f_{v,Analyt,i}$ [MN/m^2]		6,01	6,15	6,26
$f_{v,Analyt,i}$ / $f_{v,mean,i}$		101%	99%	101%

Series	i=0	i=1	i=2	i=3
$f_{v,mean,i}$ [MN/m^2]	5,08	5,29	5,08	5,52
$f_{v,Analyt,i}$ [MN/m^2]		5,27	5,44	5,59
$f_{v,Analyt,i}$ / $f_{v,mean,i}$		100%	107%	101%

Figure 9: Shear strength f_v of glulam elements with and without cracks at different levels of shear reinforcement – comparison of analytical approach with experimental results.

For the purpose of further validation, previous experiments carried out by [4] with glulam beams featuring shear reinforcement in form of fully threaded screws or screwed-in threaded rods, were calculated using the analytical method. For this comparison, all test series were utilized which complied with the prerequisites for the application of the analytical method (i.e. consistent positioning of the reinforcing elements). Furthermore, the axial slip moduli $K_{ax,ser}$, determined by the same authors [4] were applied. In the experiments, considerable increases of the shear capacity (max. 38 %) were recorded, due to the partly very high extent of reinforcement. The differences between the experimentally obtained shear capacity and the analytical results were on average below 4%. Also, the negative influence of tension stresses perpendicular to the grain on the shear strength, occurring in the case of reinforcing elements under compression, was approximated well.

3   Design of shear reinforcement for the fractured state

The analytical approach presented in chapter 2 to calculate the effectiveness of shear reinforcement, ends with the shear fracture of the timber beam. During the destructive tests it was found, that after shear fracture of the glulam element, the reinforcing elements were mostly still intact and able to carry loads, resulting in the activation of frictional resistance in the fracture plane. This finding can be considered positive with respect to the robustness of the reinforced beam: reinforcement can be designed to carry the full shear stresses parallel to the grain or tension stresses perpendicular to grain in the damaged state, preventing a full separation of the upper and lower parts of the beam in the case of a fracture. Thereby the reinforcement introduces internal redundancy since it provides a second barrier against brittle failure mechanisms, see Figure 10 and [22].
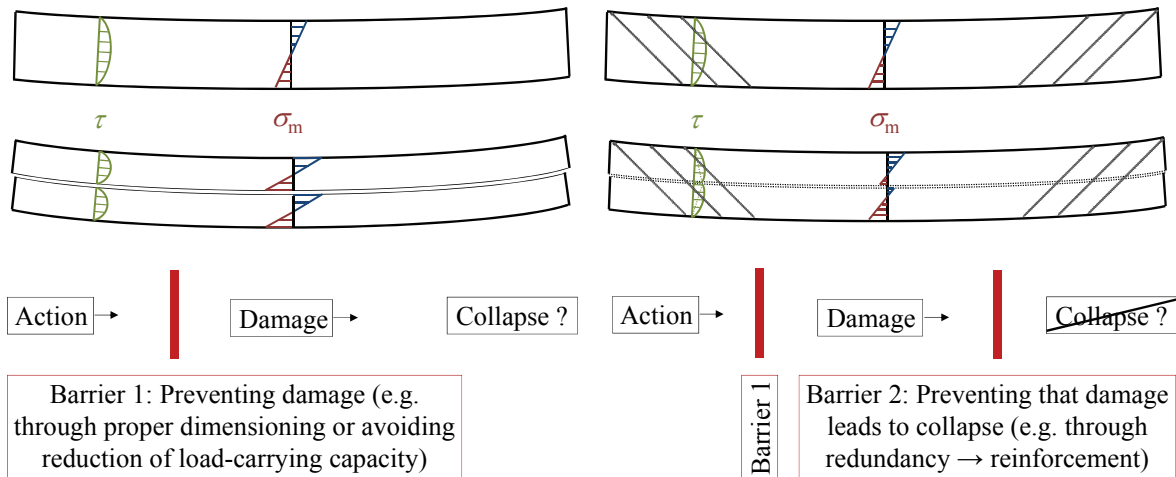
Figure 10: Barrier model in terms of robustness considerations

A method to calculate the load-carrying capacity of the two parts of the beam, mechanically jointed by reinforcing elements, is given by the shear analogy developed by Kreuzinger (e.g. [23], [24], [25] and [3]). Here, the composite section is transformed into an imaginary two-point section, featuring two levels A and B which are only coupled in terms of deflections. Level A represents the proportion of the unconnected layers to the bending rigidity of the complete section. Accordingly, the sum of bending stiffness of the individual parts is assigned to level A. The shear stiffness of level A is infinite. Level B describes the interaction of the individual parts of the cross-section due to the composite effect, i.e. the influence of shear deformation in or between the layers. Accordingly, an equivalent shear stiffness is assigned to level B which is derived from the stiffness of the fasteners/reinforcement and their distance or the shear stiffness of the layers. In addition, the bending rigidity assuming a rigid bond between the layers (parallel axis theorem) is assigned to level B. After determining the internal forces in the imaginary system, the real stresses in the individual parts of the composite section are calculated by reverse transformation. Figure 11 contains a schematic representation of the procedure.
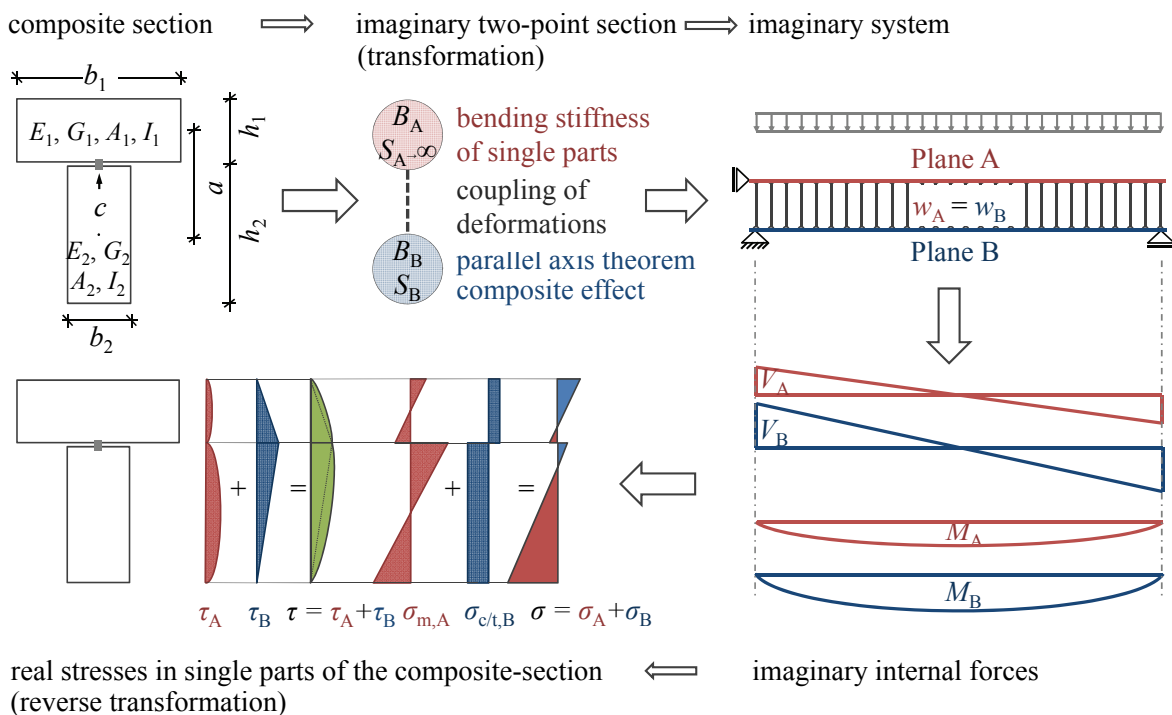

Figure 11: Schematic representation of the procedure applied in the shear analogy

The shear analogy is suitable for a computer-based implementation by means of structural analysis software. This software, e.g. 2-D frame programs, has to be able to account for shear deformation. Computer-based implementation creates the possibility of a segment-wise definition of the section properties and stiffness values. This enables the calculation of beams with varying depth and segment-wise variable stiffness of the joint between the cross-sections.

Using this method, a parametric study on curved and pitched cambered beams was performed, featuring geometries which are 1) relevant for building practice and 2) feature a high utilization rate in bending, shear and tension perpendicular to the grain. To determine the relevant geometries, all boundary conditions associated with curved and pitched cambered beams were varied in equal step sizes, whereby all relevant stress verifications were performed [1]. With predefined lower bounds (economical limit) and upper bounds (stress limits), a relevant subset was determined for each stress verification. By superimposing these subsets, the intersecting set of geometries which are relevant with regard to abovementioned objectives was determined. From this set, ten samples were selected for each beam shape (curved and pitched cambered beams). These samples covered the entire intersecting set of highly stressed geometries. For these geometries, a minimum reinforcement was determined to carry the shear flow and tension perpendicular to the grain stresses, occurring after fracture of the timber beam. Here, the approach was that the load-carrying capacity of the reinforcing elements just covered the occurring stresses, i.e. the reinforcing elements are fully utilized and placed at maximum possible distances. Due to the correlation between joint stiffness and resulting shear flow, this process is iterative. To cover the worst case in terms of bending stresses, the fracture plane was assumed to occurr at half the beam depth. A possible frictional resistance in the fracture plane was neglected. The axial slip moduli $K_{ax,ser}$ of the pre-drilled and screwed-in threaded rods were taken from [4]. Characteristic values for the load-carrying capacity of threaded rods, $F_{ax,Rk}$ and $F_{v,Rk}$, are given for example in [26]. With regard to the slip moduli K_{ser} and the necessary number of reinforcing elements to carry the occurring stresses in tension perpedicular to the grain, a standardized procedure was applied [2]. The length segment featuring reinforcements was varied between 10 % and 20 % of the total beam length, starting at the supports, so that in extreme cases the total beam length featured reinforcements (including reinforcement against tension stresses perpendicular to the grain in the curved part).

In the case of the smallest chosen length segment featuring shear reinforcement, the maximum increase of bending stresses, compared to the intact (unfractured) state, reached 33 %, see Figure 12. This can be explained by the high axial slip moduli of the threaded rods and the resulting high joint stiffness. This in turn results in high shear flows and thus - taking into account the axial load-carrying capacity of the threaded rods - in rather small distances of the reinforcing elements. At a given level of joint stiffness, an increase of the joint stiffness will only result in a highly under-proportional increase of shear flow and thus in only marginal changes of bending stresses. Between the different forms of beams, only minor differences of utilization factors could be determined. With increasing ratio $\ell/(h_{ap}$ or $h_1)$, the utilization rate slightly increased.

An increasing length of the segment featuring shear reinforcement resulted in a significantly lower increase of bending stresses in the case of fracture. Furthermore, with an increasing length of shear reinforced area, a significant change in magnitude of shear flow but only a marginal change in the sum of shear flow to be transferred was determined. Accordingly, the sum of necessary reinforcing elements increases only marginally with increasing length of the shear reinforced segment, meaning that the maximum possible distances between the reinforcing elements increase in a nearly linear manner.
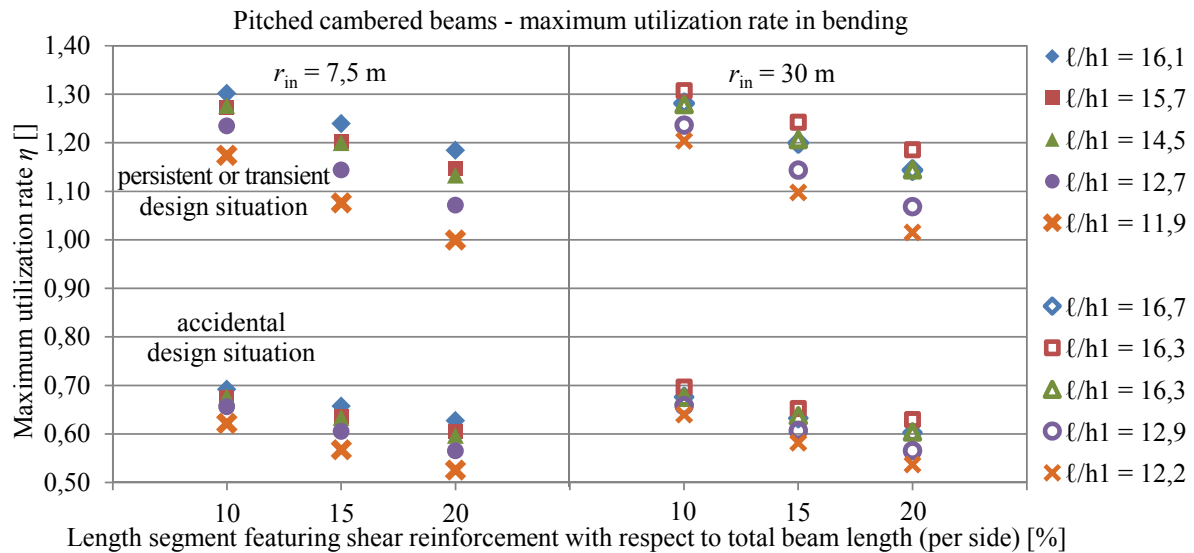
Figure 12: Exemplary results (pitched cambered beam) of the parametric study on the increase of bending stresses in the case of fracture of the glulam beam – variation of geometry and arrangement of shear reinforcement

To validate the results presented above, selected forms of curved and pitched cambered beams were calculated using the finite element method [27]. The calculations were performed using two different models, 1) a model with plane elements and spring elements to model the stiffness of the reinforcing elements and 2) a model with plane elements in which the reinforcing elements were completely modelled by beam elements, see [1] and [28] for further information. The results obtained with both models were almost identical. The beam geometries were chosen to differ greatly from the form of a straight beam, i.e. the variation of depth as well as the curvature were distinctive. The comparison was made based on the bending stresses on the top and bottom edge along the length of the beam. A comparison with the results obtained with the shear analogy showed good agreement for the areas of the beam with varying depth. In the apex area (within ca. $\pm 2 \cdot h_{ap}$) however, the differences were not negligible. They were more pronounced in the case of short lengths of shear reinforced area in comparision to longer lengths featuring shear reinforcement. The reason for the differences is mainly described by the fact that the shear analogy is derived from the beam theory, while the non-linear stress-distribution in the apex area of curved or pitched cambered beams has to be approximated by plate theory [29]. Accordingly, a significantly better fit could be achieved when the coefficients given in [29] are applied to account for the non-linear stress distribution However it should be noted that these coefficients were not derived for the given case of the fractured, mechnically jointed cross-section. In all cases, the shear analogy method provided slightly higher absolute values of maximum bending stresses, i.e. delivered results on the safe side.

4 Conclusions

An analytical approach is proposed to determine the load-carrying capacity of timber beams in the intact (unfractured) state, featuring shear reinforcement in form of threaded rods or fully threaded screws. A comparison was conducted with results from laboratory tests with reinforced glulam beams as well as with experimental data from other research institutions. This showed good agreement between the experimental shear stiffness and analytically determined stiffness as well as experimental failure load and analytically determined load-carrying capacity. The best agreement is found if the increase in shear capacity due to the interaction between shear and compression stresses perpendicular to the

grain is taken into account, in addition to the proportional load uptake of the reinforcement. The quality of the results depends on the accuracy of the input parameters (e.g. the axial slip modulus of the fully threaded screws or threaded rods) and the principles describing the effect of stress interaction on shear capacity.

Considering the intact (unfractured) state, comparative calculations of glulam elements which are reinforced by threaded rods indicate that, under realistic constructive conditions (dimensions and configuration), an increase in shear capacity of up to 20% is feasible. These calculations include a potential reduction of shear capacity of the glulam beam due to e.g. shrinkage cracks as well as the influence of relaxation effects. Preliminary investigations with respect to a further increase in shear capacity by using threaded rods show, that an examination of pre-stressed threaded rods, anchored in disc springs with degressive spring characteristics (load-deformation curves) could prove adequate. In existing structures, the upper portion of the threaded rod could be screwed or glued into the timber beam and the remaining part of the threaded rod would remain without bond. The anchorage of the lower part of the threaded rod in the disc springs could be realized by means of nuts, which could simultaneously be used for applying the pretensioning force.

With respect to internal redundancy of the reinforced beam against brittle failure mechanisms such as shear or tension perpendicular to the grain it is possible to design the reinforcing elements such that they prevent the complete separation of the upper and lower parts in the event of fracture of the beam along the grain. For the fractured beam, which is mechanically jointed by the reinforcing elements, an applicable approximation method is given by the shear analogy. This method is also applicable to curved and pitched-cambered beams in which the maximum bending stresses occur outside the apex zone. In these cases, the shear analogy method provides slightly higher absolute values of maximum bending stresses, i.e. delivers results on the safe side. Extensive comparative calculations of highly stressed shapes of glulam beams, featuring the minimum required reinforcement to carry the released stresses after fracture, show that the maximum increase in bending stresses between the intact state and the fractured state is in the range of one third. When the accidental design situation is applied for this case, it translates into a maximum utilization rate of 70%. Due to the resulting high level of joint stiffness, a change of joint stiffness will only have a minor influence on the magnitude of bending stresses. A reduction of the distance of the reinforcing elements or the use of glued-in instead of pre-drilled, screwed-in threaded rods would not lead to any noteworthy improvement of stress levels in the fractured state. However, an increasing length of the segment featuring shear reinforcement leads to significantly lower increase in bending stresses in the case of fracture of the beam along the grain. The sum of shear flow to be transferred increases only marginally. It is therefore desirable to choose an arrangement of the shear reinforcement over longer segments of the beam length since this also implicates clear benefits for construction practice due to larger possible distances between the reinforcing elements.

Literature

[1]   Dietsch, P., Einsatz und Berechnung von Schubverstärkungen für Brettschichtholzbauteile, Dissertation, Technische Universität München, 2012.

[2]   DIN 1052:2008-12, Entwurf, Berechnung und Bemessung von Holzbauwerken. Allgemeine Bemessungsregeln und Bemessungsregeln für den Hochbau, DIN, Berlin, 2008.

[3]   DIN EN 1995-1-1/NA:2010-12, Nationaler Anhang – National festgelegte Parameter – Eurocode 5: Bemessung und Konstruktion von Holzbauten – Teil 1-1: Allgemeines – Allgemeine Regeln und Regeln für den Hochbau, DIN, Berlin, 2010

[4]   Blaß, H.-J., Krüger, O., Schubverstärkung von Holz mit Holzschrauben und Gewindestangen, Karlsruher Berichte zum Ingenieurholzbau, Band 15, Universitätsverlag Karlsruhe, 2010.

[5]   Trautz, M., Koj, C., Mit Schrauben Bewehren – Neue Ergebnisse, Bautechnik, Vol. 86, No. 4, 2009, pp. 228-238.

[6]   Dietsch, P., Mestek, P., Winter, S., Analytischer Ansatz zur Erfassung von Tragfähigkeitssteigerungen infolge von Schubverstärkungen in Bauteilen aus Brettschichtholz und Brettsperrholz, Bautechnik, Vol. 89, No. 6, 2012, pp. 402-414.

[7]   EN 1995-1-1:2004, Eurocode 5: Design of timber structures – Part 1-1: General – Common rules and rules for buildings, CEN, Brussels, 2004.

[8]   Lischke, N., Zur Anisotropie von Verbundwerkstoffen am Beispiel von Brettlagenholz, Fortschritts-Bericht VDI, Reihe 5, Nr. 98, VDI-Verlag, Düsseldorf, 1985.

[9]   Klöppel, K., Schardt, R., Systematische Ableitung der Differentialgleichungen für ebene anisotrope Flächentragwerke, Stahlbau, Vol. 29, No. 2, 1960, pp. 33-43.

[10]   Lekhnitskii, S., G., Anisotropic Plates (translated from Russian by Tsai, S.,W., Cheron, T.,G.), Gordon and Breach Science Publishers, New York London Paris, 1968.

[11]   Bosl, R., Zum Nachweis des Trag- und Verformungsverhaltens von Wandscheiben aus Brettlagenholz, Dissertation, Universität der Bundeswehr, München, 2002.

[12]   Spengler, R., Festigkeitsverhalten von Brettschichtholz unter zweiachsiger Beanspruchung, Teil 1 - Ermittlung des Festigkeitsverhaltens von Brettelementen aus Fichte durch Versuche, Berichte zur Zuverlässigkeitstheorie der Bauwerke, Heft 62, LKI der TU München, 1982.

[13]   Hemmer, K., Versagensarten des Holzes der Weißtanne (Abies Alba) unter mehrachsiger Beanspruchung, Dissertation, TH Karlsruhe, 1984.

[14]   Steiger, R., Gehri, E., Interaction of shear stresses and stresses perpendicular to the grain, CIB-W18 / 44-6-2, Proceedings of the international council for research and innovation in building and construction, Working commission W18 - timber structures, Meeting 44, Alghero, Italy, 2011.

[15]   abZ. Nr. Z-9.1-705 vom 26. Januar 2009, 2K-EP-Klebstoff WEVO-Spezialharz EP 32 S mit WEVO-Wärter B 22 TS zum Einkleben von Stahlstäben in Holzbaustoffe, DIBt, Berlin, 2009.

[16]   Mestek, P., Punktgestützte Flächentragwerke aus Brettsperrholz (BSP) - Schubbemessung unter Berücksichtigung von Schubverstärkungen, Dissertation, Technische Universität München, 2011.

[17]   Blaß, H.J., Bejtka, I., Uibel, T., Tragfähigkeit von Verbindungen mit selbstbohrenden Holzschrauben mit Vollgewinde, Karlsruher Berichte zum Ingenieurholzbau, Band 4, Universitätsverlag Karlsruhe, 2006.

[18]   EN 408:2003, Timber structures - Structural timber and glued laminated timber - Determination of some physical and mechanical properties, CEN, Brussels, 2003.

[19]   abZ. Nr. Z-9.1-519 vom 07. Mai 2007, SPAX-S Schrauben mit Vollgewinde als Holzverbindungsmittel - ABC Verbindungstechnik GmbH & Co. KG, Ennepetal, DIBt, Berlin, 2007

[20]   Mestek, P., Winter, S., Konzentrierte Lasteinleitung in Brettsperrholzkonstruktionen – Verstärkungsmaßnahmen, Schlussbericht zum AiF-Forschungsvorhaben Nr. 15892, Lehrstuhl für Holzbau und Baukonstruktion, Technische Universität München 2011.

[21]   Divos, F., Tanaka, T., Nagao, H., Kato, H., Determination of shear modulus on construction size timber, Wood Science and Technology, Vol. 32, No. 6, 1998, pp. 393-402.

[22]   Dietsch, P., Robustness of large-span timber roof structures - Structural aspects, Engineering Structures, Vol. 33, No. 11, 2011, pp. 3106–3112.

[23]   Kreuzinger, H., Platten, Scheiben und Schalen – ein Berechnungsmodell für gängige Statikprogramme, Bauen mit Holz, Vol. 101, No. 1, 1999, pp. 34-39.

[24]   Kreuzinger, H., Verbundkonstruktionen, in: Holzbaukalender 2002, Bruderverlag, Karlsruhe, 2001, pp. 598-621.

[25]   Kreuzinger, H., Mechanically Jointed Beams: Possibilities of Analysis and some special Problems, CIB-W18 / 34-12-7, Proceedings of the international council for research and innovation in building and construction, Working commission W18 - timber structures, Meeting 34, Venice, Italy, 2001.

[26]   abZ. Nr. Z-9.1-777 vom 30. November 2010, Gewindestangen mit Holzgewinde als Holz-verbindungsmittel – SFS Intec GmbH, Oberursel, DIBt, Berlin, 2010.

[27]   ANSYS, Release 12.0, ANSYS Inc., Canonsburg/PA, 2010

[28]   Danzer, M., Verstärkte Brettschichtholzträger veränderlichen Querschnitts, Master Thesis, Lehrstuhl für Holzbau und Baukonstruktion, Technische Universität München 2011.

[29]   Blumer, H., Spannungsberechnungen an anisotropen Kreisbogenscheiben und Sattelträgern konstanter Dicke, Lehrstuhl für Ingenieurholzbau und Baukonstruktionen, Universität Karlsruhe, 1972/1979.